SAND2023-07304C

Predicting The Transmutation of Fuel Taggants

Elijah C. Lutz*, Jeremy M. Osborn†

*Sandia National Laboratories, PO Box 5800, Albuquerque, New Mexico 87185-1136, elutz@sandia.gov
†Sandia National Laboratories, PO Box 5800, Albuquerque, New Mexico 87185-0406, jmosbor@sandia.gov

INTRODUCTION

In the event that fuel for a nuclear reactor goes missing and the fuel is eventually recovered, the ability to trace material provenance can be an important clue as to what may have happened. While fuel still packaged in fuel assemblies or fuel rods may have obvious markings as to where the fuel originated, once the fuel is broken down into fuel pellets this process becomes much more difficult. A method to trace individual fuel pellets back to where they originated would help to alleviate this issue and help investigators.

Surface level indicators have potential weaknesses such as the ability to remove them. A way to avoid this is to introduce something to the fuel itself that cannot be removed without significant reprocessing. By adding carefully selected isotopes at various quantities one can create a sort of taggant or 'barcode' that acts as an identifier to the fuel manufacturer at a minimum and could potentially carry information such as fuel final destination, enrichment, and batch number to assist even further in investigations.

This summary will briefly discuss the selection of fuel taggants and what properties are important before diving into the transmutation of taggants throughout the fuel cycle. The summary will discuss planned and ongoing experiments to test how the taggants will survive as fuels reach various levels of burnup. The focus of the summary is on how we can model and predict the transmutation of these fuel taggants. The experiments, once complete, will allow for burnup and depletion codes to be benchmarked for future calculations.

SELECTION OF TAGGANTS

Taggants must have certain properties to ensure that they meet a few different criteria. First, the materials must be easily introduced into the fuel and not introduce adverse physical side effects (increased swelling, brittleness, etc.). Secondly, the materials must not introduce large negative reactivity into the reactor. The last criteria is that the materials must have good nuclear data. This last point is important as modeling these systems for the above reactivity and transmutation calculations requires accurate nuclear data to yield accurate results. There is also some interest in the taggants being able to survive the fuel cycle and still being traceable on the backend. While spent fuel is quite hot and does a good job of protecting itself from adversaries, the ability for the taggants to survive the fuel cycle would allow future projects to identify the history of the fuel if desired. The following analysis will focus on this aspect of the fuel taggant selection process.

As part of the Intentional Forensics Venture, multiple taggant selection workshops have taken place as the venture dials in what isotopes are most promising for use as fuel taggants. The analysis presented here utilizes the 18 priority samples identified by the venture for experimental irradiation [1]. Table 1 provides a breakdown of the selected isotopes.

Table 1. Initial isotopes selected and taggant naming scheme. [1]

Taggant	Isotope 1	Isotope 2
Ni-α	28060	28061
Ni-β	28060	28062
Mo-α	42094	42100
Mo-β	42092	42097
W-α/β	74184	74186

TRANSMUTATION OF TAGGANTS

While pre-burned fuel would be easily traced back using the fuel taggants, identifying fuel on the backend of the fuel cycle will be more challenging. The primary concern is the burn-up and burn-in of the specific taggants changing their concentrations enough to no longer be traceable. There are two methods being utilized to verify if the taggants will be traceable post irradiation.

The first method is a set of experiments being performed at Oak Ridge National Laboratory (ORNL) using the High Flux Isotope Reactor (HFIR) [1]. 18 samples containing the taggants listed in Table 2 in different concentrations will be placed in the outer beryllium reflector region in two different Vertical eXperiment Facilities (VXF). Within each VXF there are 3 radial locations with 3 axial locations each containing a sample holder. The sample holder can hold up to 6 samples stacked vertically. This allows for up to 54 samples to be irradiated per VXF. The samples are located in the radial positions closest to the core, and the axial locations crossing the midplane of the core. Each of these locations can hold 6 samples, 12 samples will be in VXF-09 with 6 samples in VXF-11. Figure 1 shows the location of VXF-09 and VXF-11 circled in red [2]. The samples will be irradiated for either 3, 5, or 6 HFIR fuel cycles.

Sandia National Laboratories
U.S. DEPARTMENT OF ENERGY NNSA
Sandia National Laboratories is a multimission laboratory managed and operated by National Technology & Engineering Solutions of Sandia, LLC, a wholly owned subsidiary of Honeywell International Inc., for the U.S. Department of Energy's National Nuclear Security Administration under contract DE-NA0003525.

Table 2. Summary of HFIR modeling and irradiation plan. [1]

Position VXF-Radial-Axial	Capsule Position	Mat #	Target	PPM	HFIR Cycles
9-2-2	1	525	Ni-α	100	3
	2	526	Mo- α	100	3
	3	527	W- α	100	3
	4	528	Ni- α	1000	3
	5	529	Mo- α	1000	3
	6	559	W- α	1000	3
9-3-2	1	543	Ni- α	100	5
	2	544	Mo- α	100	5
	3	545	W- α	100	5
	4	546	Ni-β	1000	5
	5	547	Mo- β	1000	5
	6	548	W- β	1000	5
11-2-2	1	625	Ni- α	100	6
	2	626	Mo- α	100	6
	3	627	W- α	100	6
	4	628	Ni- β	100	6
	5	629	Mo- β	100	6
	6	659	W- β	100	6

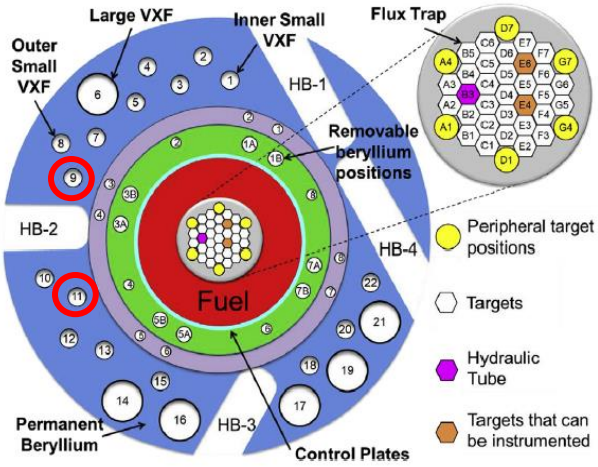

Figure 1. Diagram of HFIR irradiation facilities with VXF-9 and VXF-11 circled in red. [2]

The second method is modeling using MCNP6.2 (MCNP) with its integrated burnup capabilities to predict the transmutation of the fuel taggants. MCNP's burnup capabilities utilize CINDER90 and couples it with MCNP's KCODE calculation [3]. This allows for MCNP to calculate flux profiles in the materials of interest that are then passed to CINDER90 which performs the burnup calculation for the materials at the desired power and for the desired amount of time. These new materials are then used by MCNP to calculate a new flux profile that CINDER90 can use for the next time step. This cycle repeats for the number of time steps requested by the user on the MCNP Burn card.

The base MCNP model used for the calculations is HFIR Model Version 4.0 which is based on HFIR cycle 400 [4]. The model was modified to add the 18 samples to VXF locations as described above and outlined in Table 2. The samples are modeled as U(nat)O_2 disks that measure 0.03 cm in height and 0.3 cm in diameter. Each sample is doped with the taggants listed in Table 2. Table 2 also show the sample location, MCNP material number, and planned irradiation time. The MCNP models perform the burnup calculation for each individual sample in the 18 specified locations.

Determining the proper number of time steps to use for the MCNP burnup calculation is a time consuming process. One must balance the increased accuracy of utilizing more time steps with the large increase in computational time that includes. For each additional time step that is an active burn (i.e. not a decay only time step), two additional KCODE calculations must be run. Originally four time steps per HFIR cycle were used with 700 total KCODE cycles (throwaway and active) with 3E+6 neutron histories per cycle. After much trial and error, 8 steps per HFIR cycle, for a total of 48 cycles with the same number of KCODE cycles and 6E+6 neutron histories per cycle was the best compromise between accuracy and computational time. Time steps are shorter at the start of a HFIR cycle and extend to be longer as the cycle progresses. This allows for the shorter lived fission products to reach equilibrium in a more accurate manner.

RESULTS

Once the calculations are complete a python script is used to parse the MCNP output file and pull the results of the burnup calculation. The script pulls the data for each isotope of interest in whichever materials are specified. The script has the ability to record the data as either the mass or atom density as the value or the delta over either burnup or time depending on the users inputs. The script can output the results to a csv file if desired and plot the results for the user to view. The user can specify multiple isotopes across different materials for comparison as well.

Figure 2 shows the plot for the three Mo-Alpha 100 PPM samples. As shown in the plot Mo-100 sees a much larger change over time compared to Mo-94. This difference is due to a few reasons.

The probability of a U-235 fission resulting in Mo-100 is approximately 2E+10 times greater than that of Mo-94 when analyzing the cinder.dat file MCNP uses for fission product yields. When analyzing the various collision rates within the MCNP burnup output for these materials the Mo-99(n,g)Mo-100 reaction rates are three orders of magnitude greater than the Mo-93(n,g)Mo-94 reaction rates. Direct fission yield of Mo-100 is nine orders of magnitude greater than Mo-94.

Table 3 and Table 4 show the various reactions rates for Mo-94 and Mo-100 respectively from the last active burn time step for comparison.

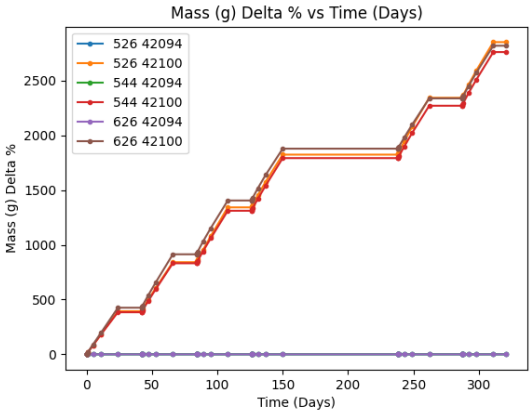

Figure 2. Mo-α 100PPM sample change in concentration over time.

Table 3. Reaction rates for Mo-94.

Reaction	Burn In (collisions/sec)	Burnup (collisions/sec)	Total (collisions/sec)
(n,g)	2.99E+03	3.32E+05	-3.29E+05
(n,2n)	3.29E+03	1.77E+00	3.29E+03
(n,3n)	0.00E+00	0.00E+00	0.00E+00
(n,α)	4.61E-11	6.17E+01	-6.17E+01
(n,p)	0.00E+00	2.18E+01	-2.18E+01
Fission Yield	9.85E-01	0.00E+00	9.85E-01
total	6.28E+03	3.32E+05	-3.26E+05

Table 4. Reaction Rates for Mo-100.

Reaction	Burn In (collisions/sec)	Burnup (collisions/sec)	Total (collisions/sec)
(n,g)	6.73E+06	1.22E+07	-5.47E+06
(n,2n)	0.00E+00	6.14E+03	-6.14E+03
(n,3n)	0.00E+00	0.00E+00	0.00E+00
(n,α)	5.05E+00	2.82E+00	2.22E+00
(n,p)	3.01E+01	1.00E-01	3.00E+01
Fission Yield	1.05E+08	0.00E+00	1.05E+08
total	1.11E+08	1.22E+07	9.93E+07

While the above reaction rates do not account for the entire difference seen in Figure 2 it is a good exercise in showing how many factors must be considered during the selection of a taggant if its ability to survive the fuel cycle is important. Another factor not considered above is radioactive decay of other fission products into the chosen isotopes.

The results for the rest of the samples can be seen in Figure 3 through Figure 7. While the remaining samples exhibit similar trends to the Mo-α model only the Mo-β model is similarly extreme with Mo-97 seeing upwards of 2000% change by the end of the irradiation. Of the Ni and W samples the highest change in concentration is around 22% for W-186 in both the W-α and W-β samples.

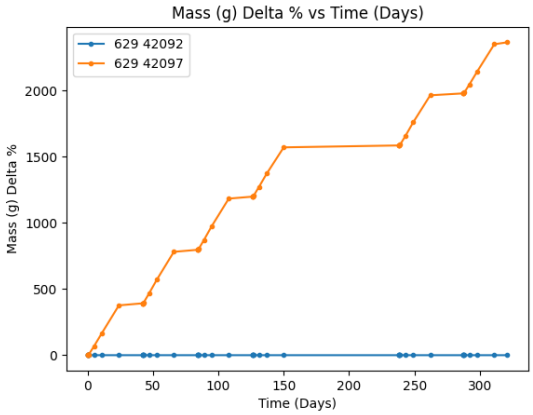

Figure 3. Mo- β 100PPM sample change in concentration over time.

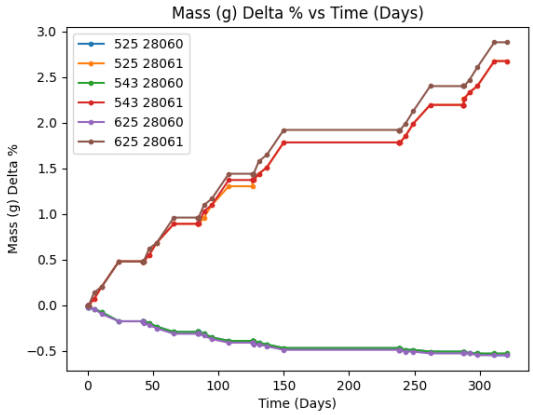

Figure 4. Ni- α 100PPM samples change in concentration over time.

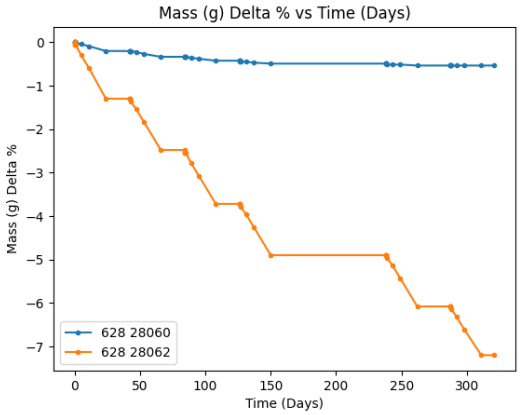

Figure 5. Ni- β 100PPM sample change in concentration over time.

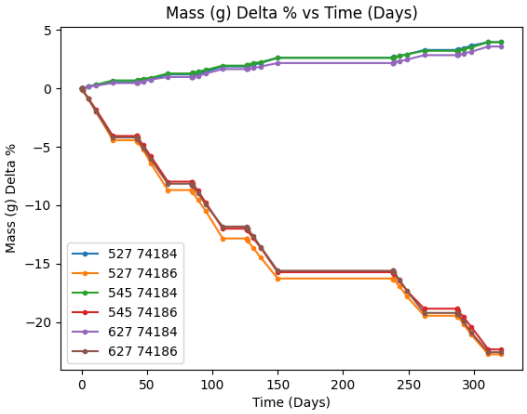

Figure 6. W- α 100PPM Samples change in concentration over time.

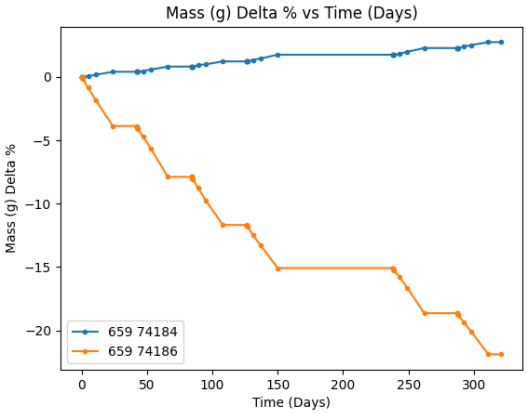

Figure 7. W- β 100PPM sample change in concentration over time.

CONCLUSIONS

Current results show a mix of promising and poor traits for transmutation throughout the fuel cycle. As shown above Mo-94, Mo-92, and Ni-60 show little change in concentration throughout the proposed irradiation in HFIR. Making them ideal candidates for this application. Mo-100 and Mo-97 conversely show over 2000% change by the end of the irradiation, meaning the original concentrations would be undeterminable at the end of the fuel cycle. The remaining isotopes sit in questionable territory and see changes in concentration ranging from less than 3% to around 22%. The experimental side of the transmutation analysis will provide a way to benchmark the above modeling results. If the model and experimental results agree it will provide increased confidence in the models and the predictive results going forwards. MCNP's burnup capabilities are rather dated as well using CINDER90 and data from ENDF-VI. Work is underway to update the cinder.dat file MCNP uses during the burnup calculation to use new data from ENDF/B-VII.1 and ENDF/B-VIII.0. There is also interest in using the experimental results to benchmark CINDER-2008 for burnup calculations. Using MCNP to get flux profiles for each sample and CINDER-2008 for the burnup calculation may result in much faster computation times with little loss in fidelity.

ACKNOWLEDGEMENTS

Sandia National Laboratories is a multimission laboratory managed and operated by National Technology & Engineering Solutions of Sandia, LLC, a wholly owned subsidiary of Honeywell International Inc., for the U.S. Department of Energy's National Nuclear Security Administration under contract DE-NA0003525. This written work is authored by an employee of NTESS. The employee, not NTESS, owns the right, title and interest in and to the written work and is responsible for its contents. Any subjective views or opinions that might be expressed in the written work do not necessarily represent the views of the U.S. Government. The publisher acknowledges that the U.S. Government retains a non-exclusive, paid-up, irrevocable, world-wide license to publish or reproduce the published form of this written work or allow others to do so, for U.S. Government purposes. The DOE will provide public access to results of federally sponsored research in accordance with the DOE Public Access Plan. SAND No. SAND2023-07304C.

The authors of this report would like to thank the U.S. Department of Energy's National Nuclear Security Administration, Office of Defense Nuclear Nonproliferation Research and Development for financial support.

The authors would also like to acknowledge the collaboration and support provided from the labs participating in the Intentional Forensics Venture. The venture team includes members from Los Alamos National Laboratory, Lawrence Livermore National Laboratory, Oak Ridge National Laboratory, Savannah River National Laboratory, Brookhaven National Laboratory, and Argonne National Laboratory.

REFERENCES

[1] S. Scott, "Intentional Forensics Venture Irradiation Experiment Sample Selection Methodology", SRNL-RP-2022-0018

[2] "High Flux Isotope Reactor (HFIR) USER GUIDE", Oak Ridge National Laboratory, 2015

[3] C. J. Werner, "MCNP Users Manual - Code Version 6.2," Los Alamos National Laboratory, report LA-UR-17-29981, 2017.

[4] N. Xoubi and R.T. Primm III, "Modeling of the High Flux Isotope Reactor Cycle 400", ORNL/TM-2004/251, ORNL, 2005